ChemComm

COMMUNICATION

A Non-Enzyme Cascade Amplification Strategy for Colorimetric Assay of Disease Biomarkers†

Received 00th January 20xx,
Accepted 00th January 20xx

DOI: 10.1039/x0xx00000x

www.rsc.org/

Jiuxing Li,[a] Zhuangqiang Gao,[ab] Haihang Ye,[a] Shulin Wan,[a] Meghan Pierce,[c] Dianping Tang[b] and Xiaohu Xia*[a]

A non-enzyme cascade amplification strategy, based on the dissolution of Ag nanoparticles and Pt nanocubes-catalyzed reaction, for colorimetric assay of disease biomarkers was developed. This strategy overcomes the intrinsic limitations of enzymes involved in conventional enzymatic amplification techniques, thanks to the utilization of noble-metal nanostructures with superior properties.

Diagnostic technologies for disease biomarker detection have become a critical component in biomedical research and clinical care.[1-4] Over the past several decades, a variety of technologies based on different signal-transducer principles have been actively explored, with notable examples including fluorescent,[5-7] chemiluminescent,[8,9] colorimetric,[10-12] electrochemical,[13,14] Raman,[15-17] and plasmonic[18,19] assays. Among them, enzyme-based colorimetric assays (in which enzymes are pre-conjugated to bioreceptors and specifically generate color signal by catalyzing chromogenic substrates) continue to receive increasing interest because of their simplicity and cost effectiveness.[20-22] In particular, they could be performed by less-trained personnel with low-cost devices, making them extremely desirable for diagnostics in resource-limited settings.

Nevertheless, extensive application of colorimetric assays in clinical diagnosis is largely limited by their relatively low detection sensitivity. A general strategy to enhance the sensitivity is to amplify color signal by assembling as many enzymes as possible on carriers (*e.g.*, polymers and nanoparticles).[23,24] However, this strategy is ultimately confined by the loading amount of enzymes on a carrier with limited space and the steric hindrance.[25] Recently, enzyme cascade amplification has emerged to be a novel and efficient signal amplification strategy for sensitivity enhancement.[26-32] A typical mechanism involves sequential cascade reactions catalyzed by enzymes – the products generated from a primary enzyme associated with bioreceptors catalyze the activation of a secondary enzyme, which in turn yields another product with drastically increased amount. While this amplification technique is highly efficient, it is subjected to a number of variables such as enzymatic activity, stability, and activation conditions. Particularly, the relatively poor stability of enzymes makes the enzyme cascade amplification system hardly survive harsh environments, which is oftentimes the case for field work and point-of-care tests.[33]

In this work, we report a non-enzyme cascade amplification (NECA) strategy for enhancing the sensitivity of colorimetric assay. This strategy lies in the dense atom packing in silver (Ag) nanoparticles and the ultrahigh catalytic activity of platinum (Pt) nanocatalysts. The NECA assay adopts the classic enzyme-linked immunosorbent assay (ELISA) platform,[20] ensuring the simplicity of the assay without the involvement of additional equipment. Specifically, as shown in Fig. 1, after antibodies-conjugated Ag nanoparticles are captured by biomarkers in a 96-well microtiter plate and uncaptured ones removed, the nanoparticles are dissolved into individual Ag^+ ions through chemical etching by H_2O_2.[34] The Ag^+ ions could then effectively inhibit the catalytic activity of Pt nanocubes as artificial

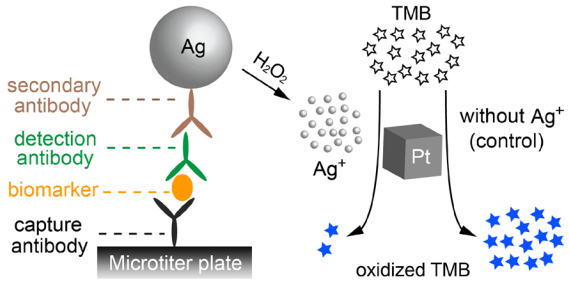

Fig. 1 Schematics showing the non-enzyme cascade amplification (NECA) strategy for disease biomarker detection.

[a] Department of Chemistry, Michigan Technological University, Houghton, Michigan 49931, United States. E-mail: xiaxh@mtu.edu
[b] Key Laboratory of Analysis and Detection for Food Safety (Fujian Province & Ministry of Education), Collaborative Innovation Center of Detection Technology for Haixi Food Safety and Products (Fujian Province), Department of Chemistry, Fuzhou University, Fuzhou 350108, People's Republic of China.
[c] Department of Chemical Engineering, Michigan Technological University, Houghton, Michigan 49931, United States.

† Electronic Supplementary Information (ESI) available: Information on materials, experimental details, and additional figures. See DOI: 10.1039/x0xx00000x

peroxidases, thereby largely eliminating the generation of blue colored products, oxidized TMB, catalyzed from 3,3',5,5'-tetramethylbenzidine (TMB, a typical peroxidase substrate).[35,36] Despite miniature in size, Ag nanoparticles consist of thousands to millions of Ag atoms that can be conveniently released in the form of Ag^+ ions. For example, the Ag nanosphere of 20 nm we used in this study (will be specified later) contains ~2.5×10^5 Ag atoms. On the other hand, as demonstrated in our recent study,[36] a single Ag^+ ion could inhibit the generation of ~10^4 oxidized TMB within several minutes owing to the superior catalytic activity of Pt nanocubes and the efficient inhibition of Ag^+ towards the catalytic reaction. Notably, the oxidized TMB possesses a large molar extinction coefficient (ε) at the level of 10^4 $M^{-1}\cdot cm^{-1}$,[37] ensuring a distinct change in color signal. Taken these two cascade processes together, the detection signal (refers to as the diminished color signal relative to a control) in the NECA system could be amplified by orders of magnitudes. Significantly, both Ag nanoparticles and Pt nanocubes are made of inert noble metals with good stabilities, making the NECA system less vulnerable to the environment.

We first conducted a set of experiments to demonstrate the feasibility and optimize the conditions of the NECA system, in which the response of Ag nanoparticles with various amounts was investigated. Specifically, 50 μL aqueous suspensions of citrate-capped Ag nanospheres with an average diameter of ~20 nm (Sigma Aldrich, Fig. 2a) were etched with 50 μL of H_2O_2 to form Ag^+ solution. Then, to the etching solution, 20 μL of Pt nanocubes with an average edge length of 7.3 nm (100 pM in particle concentration, Fig. 2b) and 100 μL of TMB substrate solution were sequentially added. Here, the Pt nanocubes were

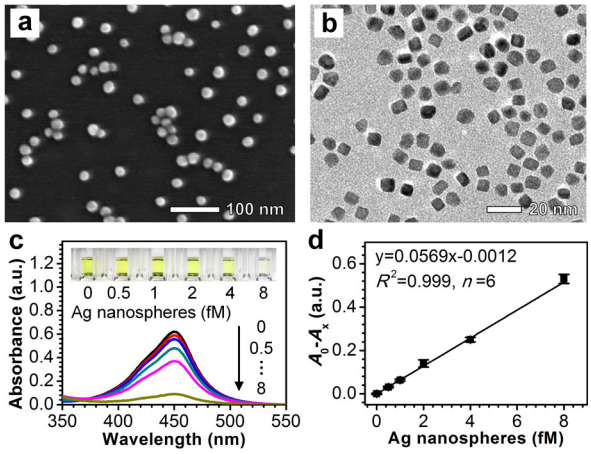

Fig. 2 Demonstration of the NECA system by varying the amount of Ag nanospheres in aqueous suspension. (a) Scanning electron microscopy (SEM) image of the 20 nm Ag nanospheres; (b) Transmission electron microscopy (TEM) image of the 7.3 nm Pt nanocubes; (c) UV-vis spectra taken from reaction solutions containing Pt cubes, TMB substrate, and Ag nanospheres of various concentrations after they had been etched by H_2O_2. The group of "0 fM Ag nanospheres" is referred to as "control". The inset shows a typical photograph of corresponding samples in cuvettes; (d) Calibration curve of (c) that was generated by plotting the decrease of absorbance at 450 nm relative to the control ($A_0 - A_x$) as a function of the Ag nanosphere concentration.

synthesized according to our recently published procedure.[35] The catalytic reaction was finally quenched by H_2SO_4, in which oxidized TMB was converted to yellow-colored diimine with λ_{max} ≈ 450 nm and ε = 5.9 × 10^4 $M^{-1}\cdot cm^{-1}$ (see the ESI† for experimental details).[38] We chose these Ag nanospheres for demonstration because: *i*) they could be easily functionalized with antibodies through electrostatic interactions;[39] *ii*) they could be prepared with good uniformities in terms of both shape and size, ensuring good reproducibility of the assay; and *iii*) they are commercially available, making it convenient to assemble the assay system for practical use. After systematic examination of various parameters (see Fig. S1 in the ESI†), the optimal conditions for etching of Ag nanospheres was found to be 0.1 M H_2O_2, 37 °C, and 20-minute incubation, at which Ag atoms in the nanospheres were almost completely converted to Ag^+ ions. It should be emphasized that, while we adopted etching at 37 °C as a standard condition in this study, the etching efficiency at 22 °C was similar to the case of 37 °C (see Fig. S1c), indicating potential use of the present system at room temperature. As shown in Fig. 2c, the intensity of color signal from the system decreased as the concentration of Ag nanospheres increased. A linear relationship was found between the decrease of absorbance at 450 nm relative to the control (A_0-A_x) and the concentration of Ag nanospheres with a range of 0.5-8.0 fM (Fig. 2d). It is worth noting that the decrease of color signal was even evident when the concentration of Ag nanospheres was as low as 0.5 fM (corresponding to only ~1.5 × 10^4 particles in a 50 μL suspension). In other words, a small amount of Ag nanospheres could induce a detectable color change, implying a high sensitivity of the system. These results clearly demonstrated the capabilities of signal amplification and quantification for the proposed NECA strategy.

We then applied the NECA system to the detection of human prostate-specific antigen (PSA) according to the principle shown in Fig. 1 (experimental details in the ESI†). PSA is the key biomarker that indicates the recurrence of prostate cancer after treatment.[40] It is pivotal to detect minute concentrations of PSA at early stages to improve survival rates of patients who have undergone radical prostatectomy.[41,42] For comparison, we benchmarked the NECA assay against conventional horseradish peroxidase (HRP) based ELISA by using the same set of antibodies and materials. Herein, antibodies were conveniently functionalized on Ag nanospheres

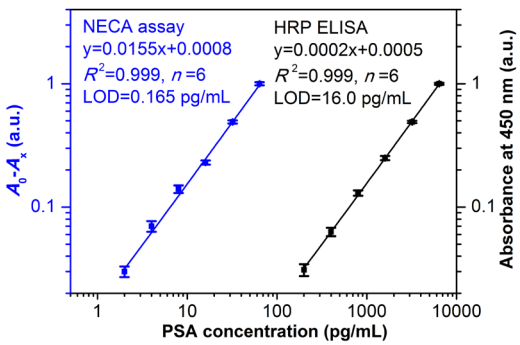

Fig. 3 Calibration curves of the NECA assay and HRP ELISA for PSA detection. Error bars indicate the standard deviations of six independent measurements.

through a simple incubation process (see the ESI†), ensuring the simplicity of the NECA assay.

PSA standards of various concentrations were tested by both assays and quantified using a microtiter plate reader. For the NECA assay (Fig. 3, blue), a quality linear relationship (R^2=0.999) in the range of 2-64 pg/mL PSA was found by plotting the decrease of absorbance relative to the control (A_0-A_x) against PSA concentration. The coefficient of variations (n = 6) across the entire concentration range were determined to be <10%, indicating a good reproducibility of the assay. The limit of detection (LOD),[43,44] defined as the concentration corresponding to a siganl that is three times the standard deviation of zero calibrator, was calculated to be 0.165 pg/mL. In comparison, a linear range of 200-6,400 pg/mL and a LOD of 16.0 pg/mL PSA were determined for the conventional HRP ELISA based on its calibration curve (Fig. 3, black). These results suggest that the NECA system could enhance detection sensitivity by approximately 2 orders of magnitude as compared to conventional ELISA. Significantly, this substantial enhancement of sensitivity does not compromise the simplicity of colorimetric assay since the NECA system shares the same platform and similar procedure with conventional ELISA. It is worth mentioning that the utilized amounts of Ag nanospheres and Pt nanocubes were tiny based on the detection procedure (*i.e.*, ~2.0×10^{-6} and ~1.0×10^{-8} gram per test, respectively. See ESI†). Therefore, even though precious noble metals are used in the NECA system, their costs in individual tests are negligible.

We also investigated the effect of Ag nanosphere size on the detection sensitivity of NECA for PSA. Specifically, we have examined the performance of two additional batches of Ag nanosphere from Sigma Aldrich (with average diameters of 10 nm and 40 nm, see Fig. S2a, b) in detecting PSA standards. The detection procedures were kept the same as the standard procedure used for 20 nm Ag sphere, except for the substitution of 20 nm Ag spheres with the same amount of 10 nm or 40 nm Ag sphere. As shown by Fig. S2c, d, the detection sensitivities of 10 nm and 40 nm Ag spheres were determined to be 0.195 pg/mL and 0.549 pg/mL, respectively (*versus* 0.165 pg/mL for 20 nm Ag spheres). It can be concluded that: *i*) decreasing the size of Ag sphere from 20 to 10 did not cause apparent change in detection sensitivity. This observation might be explained by the argument that 10 nm Ag sphere were more efficient in binding to analytes, which compensated their relatively smaller amount of Ag element caused by size reduction; and *ii*) increasing the size of Ag sphere from 20 to 40 nm decreased the detection sensitivity by approximately 3.3 times. This decrease of sensitivity may be ascribed to the enhanced steric hindrances of antibodies labeled on Ag spheres.[45,46]

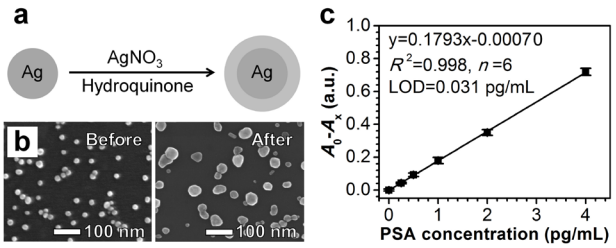

Fig. 4 Silver enhancement technique-coupled NECA assay. (a) Schematics showing the treatment of Ag nanospheres with silver enhancement; (b) SEM images of the 20 nm Ag nanospheres before and after silver enhancement; (c) Calibration curve of silver enhancement technique-coupled NECA assay for PSA detection.

To evaluate the stability of the NECA system, we heated the two critical components – Ag nanospheres and Pt nanocubes – at high temperatures (up to 90 °C) for 6 hours prior to the assay of a 10 pg/mL PSA standard. As shown by Fig. S3 (see ESI†), no significant change in both detection sensitivity and reproducibility was observed for the NECA assay after the Ag and Pt particles had been treated with heat. This superior stability might be ascribed to the inherent inertness of noble metals.[25] In this regard, the NECA system is expected to be more reliable for detection at extreme conditions compared to enzyme-based signal amplification techniques.

It is worthy to emphasize that sensitivity of the NECA system could be further enhanced by coupling with other cascade mechanisms. For example, we have demonstrated that the sensitivity could be improved by the "silver enhancement" technique (Fig. 4a), which is widely used in bioanalysis.[47,48] Herein, Ag nanospheres act as catalysts to reduce Ag^+ ions (from $AgNO_3$) to metallic Ag at room temperature in the presence of hydroquinone as a reducing agent. As shown by the SEM images in Fig. 4b, the 20 nm Ag nanospheres were enlarged to ~50 nm during the silver enhancement process, with which Ag element was greatly enriched. By integrating this technique to the NECA system (see the ESI† for details), the LOD of PSA assay was lowered to 0.031 pg/mL as calculated on the basis of its calibration curve (Fig. 4c). It can be concluded that, although the system has not yet been optimized for maximum Ag enrichment, an additional 5-fold enhancement in sensitivity relative to the standard NECA assay could be achieved.

Finally, in order to demonstrate the potential use of the NECA assay in clinical scenarios, we applied it to detecting human serum samples spiked with PSA standard at different concentrations in range of 5–50 pg/mL. As shown in Table S1 (see ESI†), the analytical recoveries (defined as the amount measured as a percentage of the amount of PSA originally added to a sample[25]) for the five PSA spiked human serum samples were determined to be in the range of 92.46-104.31 %. The coefficient of variation (n = 6) for all samples was below 10.91 %. We also benchmarked the detection against a commercial ELISA kit (Abcam plc., United Kingdom). As shown in Fig. 5, the detection results from the NECA assay and ELISA kit correlated very well with a correlation coefficient R^2 = 0.993. These results indicated that the performance of the NECA system was essentially not compromised by the complex matrices in human serum, suggesting the potential application of this technique in clinical diagnostics.

In conclusion, we have demonstrated a non-enzyme cascade signal amplification strategy for colorimetric assay of disease biomarkers with substantially enhanced sensitivity. This strategy was built by integrating two cascade processes – dissolution of nanoscale Ag particles to individual Ag^+ ions and generation of colored molecules catalyzed by Pt nanocubes as artificial peroxidases. To our knowledge, such a non-enzyme cascade amplification strategy has never been demonstrated

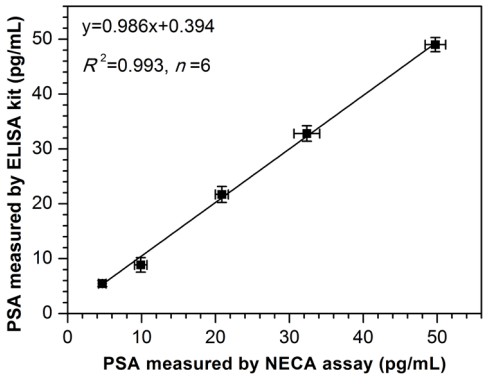

Fig. 5 Correlation analysis between the NECA assay and a commercial ELISA kit (ab188389, Abcam plc.) in quantifying PSA from five PSA-spiked serum samples. Error bars indicate the standard deviations of six independent measurements.

before. Significantly, this technique is compatible with the instrument and procedures of exiting biosensing technologies, making it straightforward to employ it for clinical diagnostics. The concept of non-enzyme cascade signal amplification presented here may open up a new avenue for the development of more sensitive and reliable diagnostic technologies.

This work was supported by the National Science Foundation (NSF) Career Award (CHE-1651307), the Portage Health Foundation (PHF) research fund, and the startup funds from Michigan Technological University.

Notes and references

1. D. A. Giljohann and C. A. Mirkin, *Nature*, 2009, **462**, 461-464.
2. A. P. F. Turner, *Chem. Soc. Rev.*, 2013, **42**, 3184-3196.
3. W. Zhou, X. Gao, D. Liu and X. Chen, *Chem. Rev.*, 2015, **115**, 10575-10636.
4. B. A. Kairdolf, X. Qian and S. Nie, *Anal. Chem.*, 2017, **89**, 1015-1031.
5. C. Y. Zhang, H. C. Yeh, M. T. Kuroki and T. H. Wang, *Nat. Mater.*, 2005, **4**, 826-831.
6. L. Zhang, S. Guo, S. Dong and E. Wang, *Anal. Chem.*, 2012, **84**, 3568-3573.
7. R. Hu, T. Liu, X.-B. Zhang, S.-Y. Huan, C. Wu, T. Fu and W. Tan, *Anal. Chem.*, 2014, **86**, 5009-5016.
8. Z. Yang, H. Liu, C. Zong, F. Yan and H. Ju, *Anal. Chem.*, 2009, **81**, 5484-5489.
9. H. Akhavan-Tafti, D. G. Binger, J. J. Blackwood, Y. Chen, R.S. Creager, R. de Silva, R.A. Eickholt, J. E. Gaibor, R. S. Handley and K. P. Kapsner, et al. *J. Am. Chem. Soc.*, 2013, **135**, 4191-4194.
10. Q. Zhang, B. Zhao, J. Yan, S. Song, R. Min and C. Fan, *Anal. Chem.*, 2011, **83**, 9191-9196.
11. J.-S. Lee, P. A. Ulmann, M. S. Han and C. A. Mirkin, *Nano Lett.*, 2008, **8**, 529-533.
12. S. Wignarajah, G. A. R. Y. Suaifan, S. Bizzarro, F. J. Bikker, W. E. Kaman and M. Zourob, *Anal. Chem.*, 2015, **87**, 12161-12168.
13. D. Lu, J. Wang, L. Wang, D. Du, C. Timchalk, R. C. Barry and Y. Lin, *Adv. Funct. Mater.*, 2011, **21**, 4371-4378.
14. A. Abellán-Llobergat, I. Jeerapan, A. Bandodkar, I. Vidal, A. Canals, J. Wang and E. Morallon, *Biosens. Bioelectron.*, 2017, **91**, 885-891.
15. X. Zhang, M. A. Young, O. Lyandres and R. P. Van Duyne, *J. Am. Chem. Soc.*, 2005, **127**, 4484-4489.
16. C. Costas, V. Lopez-Puente, G. Bodelon, C. González-Bello, J. Perez-Juste, I. Pastoriza-Santos and L. M. Liz-Marzan, *ACS Nano*, 2015, **9**, 5567-5576.
17. J. Li, Z. Zhu, B. Zhu, Y. Ma, B. Lin, R. Liu, Y. Song, S. Tu and C. Yang, *Anal. Chem.*, 2016, **88**, 7828-7836.
18. S. M. Tabakman, L. Lau, J. T. Robinson, J. Price, S. P. Sherlock, H. Wang, B. Zhang, Z. Chen, S. Tangsombatvisit, J. A. Jarrell, P. J. Utz, and H. Dai, *Nat. Commun.*, 2011, **2**, 466.
19. R. De La Rica and M. M. Stevens, *Nat. Nanotechnol.*, 2012, **7**, 821-824.
20. R. M. Lequin, *Clin. Chem.*, 2005, **51**, 2415-2418.
21. C.-M. Cheng, A. W. Martinez, J. Gong, C. R. Mace, S. T. Phillips, E. Carrilho, K. A. Mirica and G. M. Whitesides, *Angew. Chem., Int. Ed.*, 2010, **49**, 4771-4774.
22. M. R. Wick, *Ann. Diagn. Pathol.*, 2012, **16**, 71-78.
23. A. Ambrosi, F. Airo and A. Merkoçi, *Anal. Chem.*, 2010, **82**, 1151-1156.
24. J. Lin, Y. Liu, J. Huo, A. Zhang, Y. Pan, H. Bai, Z. Jiao, T. Fang, X. Wang, Y. Cai, Q. Wang, Y. Zhang and X. Qian, *Anal. Chem.*, 2013, **85**, 6228-6232.
25. H. Ye, K. Yang, J. Tao, Y. Liu, Q. Zhang, S. Habibi, Z. Nie and X. Xia, *ACS Nano*, 2017, **11**, 2052-2059.
26. B. Zou, Y. Ma, H. Wu and G. Zhou, *Angew. Chem., Int. Ed.*, 2011, **50**, 7395-7398.
27. Z. Gao, L. Huo, M. Xu and D. Tang, *Sci. Rep.*, 2014, **4**, 3966.
28. J. Yin, T. Xu, N. Zhang and H. Wang, *Anal. Chem.*, 2016, **88**, 7730-7737.
29. E. Kim, P. D. Howes, S. W. Crowder and M. M. Stevens, *ACS Sens.*, 2017, **2**, 111-118.
30. L. Qiu, Y. Zhang, C. Liu and Z. Li, *Chem. Commun.*, 2017, **53**, 2926-2929.
31. L.-J. Wang, M. Ren, Q. Zhang, B. Tang and C.-Y. Zhang, *Anal. Chem.*, 2017, **89**, 4488-4494.
32. L. Ge, W. Wang, X. Sun, T. Hou and F. Li, *Anal. Chem.*, 2016, **88**, 2212-2219.
33. H. Wei and E. Wang, *Chem. Soc. Rev.*, 2013, **42**, 6060-6093.
34. Q. Zhang, C. M. Cobley, J. Zeng, L.-P. Wen, J. Chen and Y. Xia, *J. Phys. Chem. C*, 2010, **114**, 6396-6400.
35. H. Ye, Y. Liu, A. Chhabra, E. Lilla and X. Xia, *ChemNanoMat*, 2017, **3**, 33-38.
36. Z. Gao, G. G. Liu, H. Ye, R. Rauschendorfer, D. Tang and X. Xia, *Anal. Chem.*, 2017, **89**, 3622-3629.
37. L. Gao, J. Zhuang, L. Nie, J. Zhang, Y. Zhang, N. Gu, T. Wang, J. Feng, D. Yang and S. Perrett, *Nat. Nanotechnol.*, 2007, **2**, 577-583.
38. P. D. Josephy, T. Eling and R. P. Mason, *J. Biol. Chem.*, 1982, **257**, 3669-3675.
39. G. T. Hermanson, *Bioconjugate Techniques*, 2nd ed.; Academic Press: San Diego, 2008.
40. D. M. Rissin, C. W. Kan, T. G. Campbell, S. C. Howes, D. R. Fournier, L. Song, T. Piech, P. P. Patel, L. Chang, A. J. Rivnak, E. P. Ferrell, J. D. Randall, G. K. Provuncher, D. R. Walt and D. C. Duffy, *Nat. Biotechnol.*, 2010, **28**, 595-599.
41. B. Laxman, D. S. Morris, J. Yu, J. Siddiqui, J. Cao, R. Mehra, R. J. Lonigro, A. Tsodikov, J. T. Wei, S. A. Tomlins and A. M. Chinnaiyan, *Cancer Res.*, 2008, **68**, 645-649.
42. D. M. Rissin, C. W. Kan, T. G. Campbell, S. C. Howes, D. R. Fournier, L. Song, T. Piech, P. P. Paterl, L. Chang, A. J. Rivnak, E. P. Ferrell, J. D. Randall, G. K. Provuncher, D. R. Walt and D. C. Duffy, *Nat. Biotechnol.*, 2010, **28**, 595-599.
43. D. A. Armbruster, M. D. Tillman and L. M. Hubbs, *Clin. Chem.*, 1994, **40**, 1233-1238.
44. D. A. Armbruster and T. Pry, *Clin. Biochem. Rev.*, 2008, **29**, S49-S52.
45. K. Kaur and J. A. Forrest, *Langmuir*, 2012, **28**, 2736-2744.
46. Q. Ju, M. O. Noor and U. J. Krull, *Analyst*, 2016, **141**, 2838-2860.
47. S. Gupta, S. Huda, P. K. Kilpatrick and O. D. Velev, *Anal. Chem.*, 2007, **79**, 3810-3820.
48. T. A. Taton, C. A. Mirkin and R. L. Letsinger, *Science*, 2000, **289**, 1757-1760.